SAND2019-5975C

Dynamic Tensile Behavior of Soft Ferromagnetic Alloy Fe-Co-2V

2019 SEM Annual Conference and Exposition on Experimental and Applied Mechanics, Reno, NV, June 3-6, 2019

PRESENTED BY

Brett Sanborn, Bo Song, Don Susan, Kyle Johnson, Jeff Dabling, Jay Carroll, Adam Brink, Scott Grutzik, and Andrew Kustas

SAND ##########
(Unclassified Unlimited Release)

Sandia National Laboratories is a multimission laboratory managed and operated by National Technology & Engineering Solutions of Sandia, LLC, a wholly owned subsidiary of Honeywell International Inc., for the U.S. Department of Energy's National Nuclear Security Administration under contract DE-NA0003525.

Background

Fe-Co-2V alloys have the **highest available magnetic saturation** of any commercial soft alloys

- **Saturation** is the state reached when an increase in applied magnetic field ***cannot increase*** magnetization of the material further

Fe-Co-2V is used in solenoids, electric motors, and other components

Common commercial alloys:

- **Permendur 2V** – (Manufactured by Metalwerks, Inc.)
- **Hiperco 50A** (Hiperco is a tradename of Carpenter Technologies Inc.)

Example:

- Aircraft Auxiliary Power Unit (**APU**) and Ram Air Turbine (**RAT**) generators use Fe-Co-2V alloy
- **Generate** (RAT) and **supply** (APU) power in emergency situations (engine failure) for cockpit instrumentation and flight controls (power is typically generated in main fuel-burning engines)
- Fe-Co-2V alloy maximizes power generation for a given weight

Understanding mechanical behavior is critical for design and simulation of different scenarios

Background

Discontinuous yielding:
Lüders Banding

Linear hardening

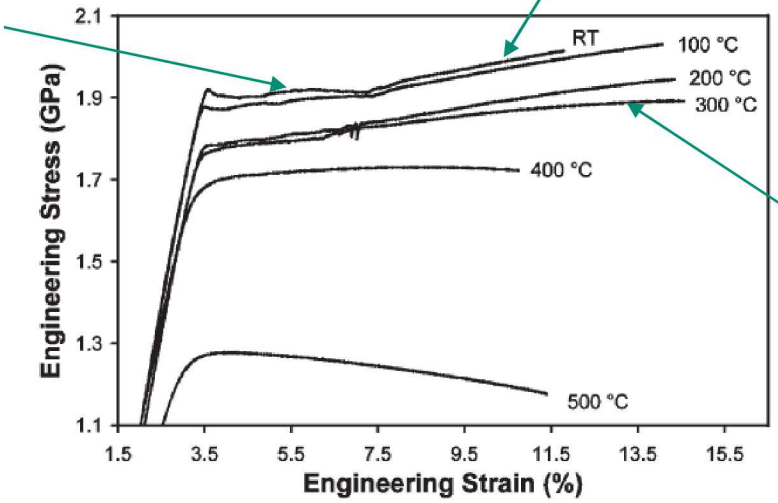

Temperature Dependent Work Hardening Rate

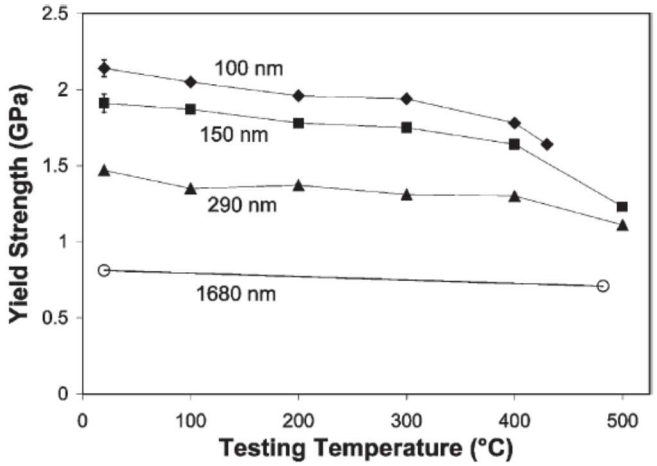

Yield strength depends on grain size (Hall-Petch behavior)

Only **two** quasi-static studies have been done

- Special small grain sizes only
- High temperature only
- Rate effect seen even in quasi-static regime

How would a commercial alloy perform under abnormal mechanical conditions?

- Drop/impact loading rates?
- Cold temperatures?

This information is needed to make and improve modeling and simulation of applications

Duckham, A., Zhang, D.Z., Liang, D., Luzin, V., Cammarata, R.C., Leheny, R.L., Chien, C.L., and Weihs, T.P., 2003, Temperature dependent mechanical properties of ultra-fine grained FeCo-2V, *Acta Materialia*, 51:4083-4093.

Experimental Matrix

Strategy: Use Kolsky tension bar and Drop-Hopkinson bar to measure tensile stress-strain behavior over -100 to 100°C

Nominal Strain Rate (s^{-1})	Temperature (°C)	Apparatus
40	20 (ambient)	Drop-Hopkinson Bar
65	-100	Kolsky Tension Bar
110	20 (ambient)	Drop-Hopkinson Bar
230	-100	Kolsky Tension Bar
230	-50	Kolsky Tension Bar
230	20 (ambient)	Kolsky Tension Bar
230	100	Kolsky Tension Bar

Kolsky Tension Bar Experimental Setup

Ambient temperatures:

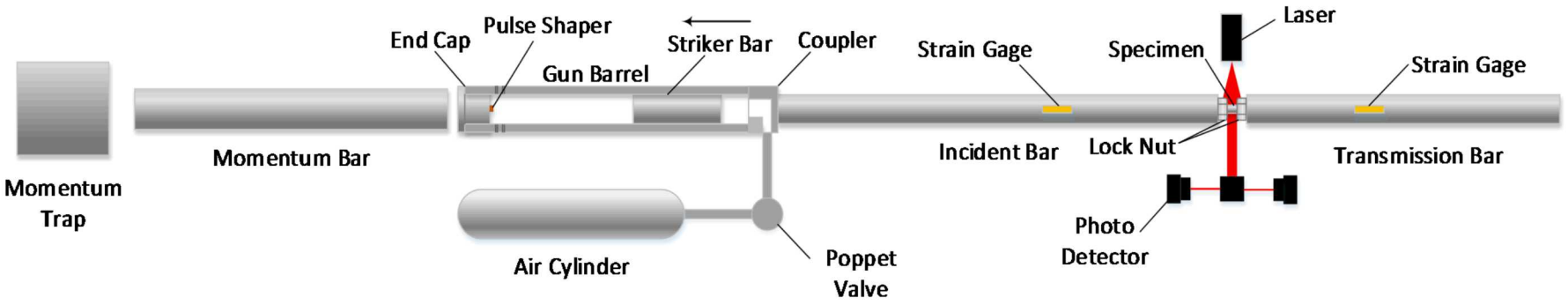

High/low temperatures:

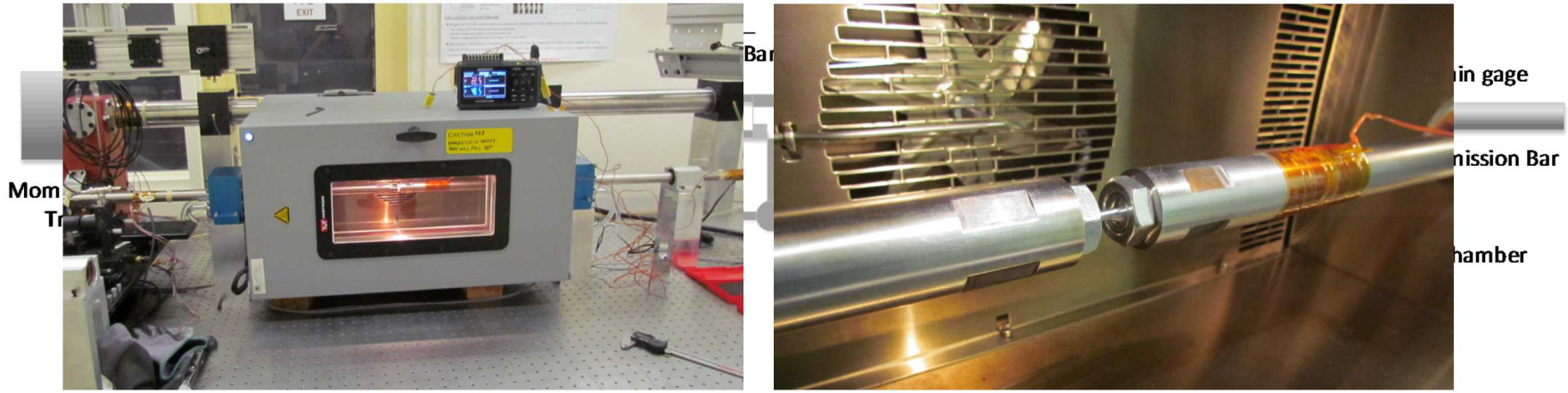

Drop-Hopkinson Bar Experimental Setup

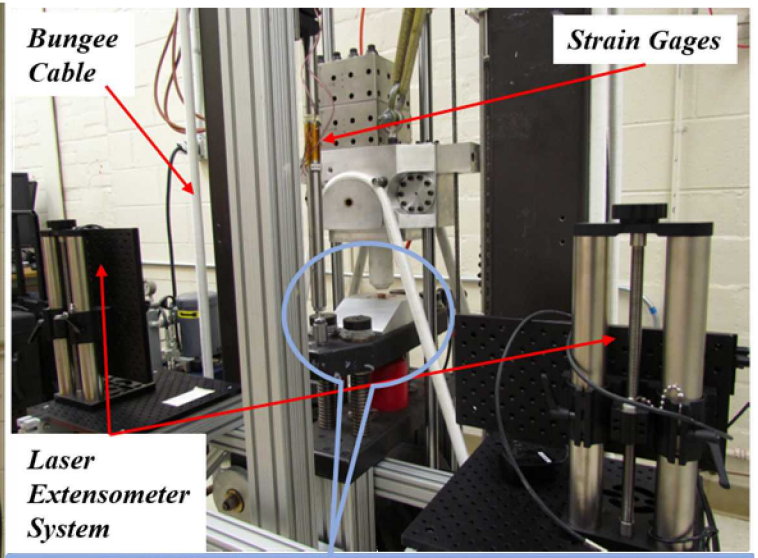

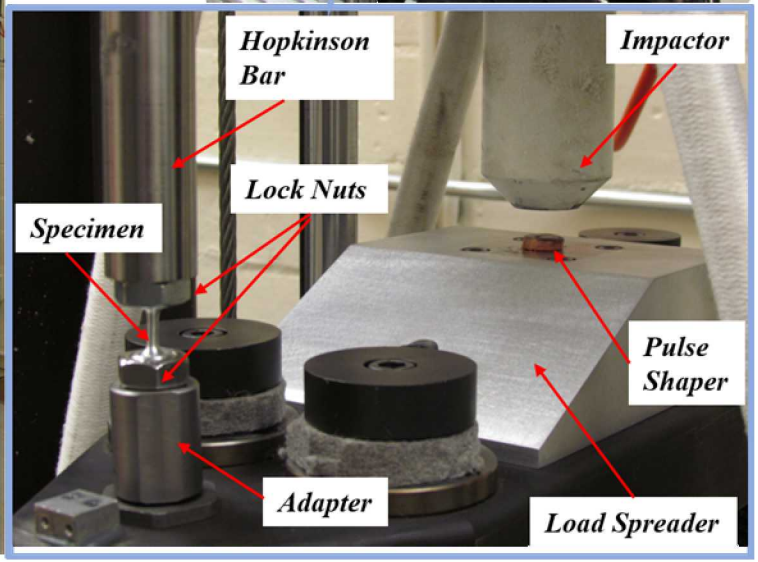

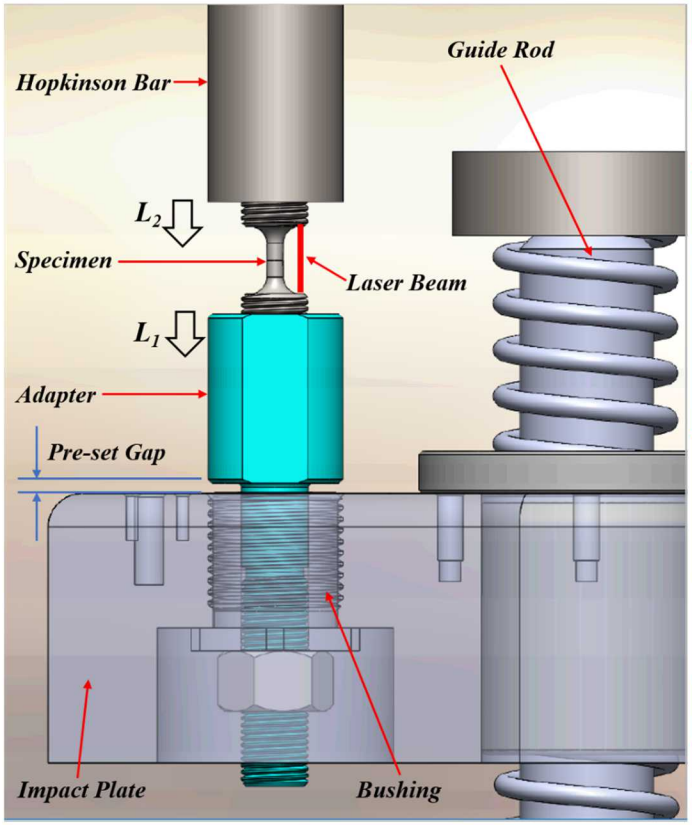

Strain Correction Method

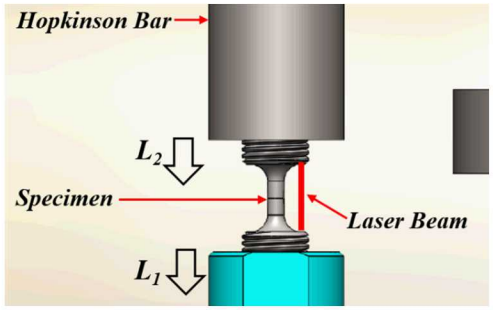

- For both Kolsky and DH Bar, strain is overestimated due to the measurement location
- Strain correction is needed only to include the straight part of the specimen
- Shoulder deforms plastically due to hardening in the material

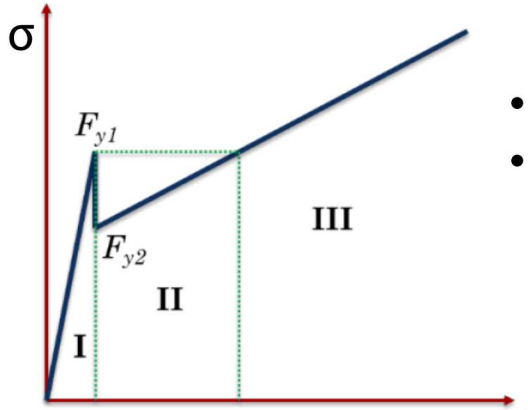

- Three-region correction method will be presented by Bo Song
- Uses laser displacements, force output, and specimen geometry to correct the measured strain

$$\varepsilon = \begin{cases} c' \cdot \dfrac{L_1 - L_2}{L_s} & \text{(Region I)} \\ \dfrac{L_1 - L_2}{L_s} - \dfrac{F}{E_s \cdot \pi \cdot r_0^2} \cdot \left(\dfrac{1}{c'} - 1 \right) & \text{(Region II)} \\ \dfrac{F_{y1}}{E_s \cdot \pi \cdot r_0^2} + \dfrac{L_1 - L_2 - \dfrac{2 \cdot F}{E_s \cdot \pi} \cdot \int_{x_0}^{x_l} \dfrac{dx}{\left(R + r_0 - \sqrt{R^2 - x^2} \right)^2} - \dfrac{F_{y1}}{E_s \cdot \pi \cdot r_0^2} \cdot (2x_0 + L_s)}{\dfrac{2 \cdot F \cdot r_0^2 \cdot \int_0^{x_0} \dfrac{dx}{\left(R + r_0 - \sqrt{R^2 - x^2} \right)^2} - 2 \cdot F_{y2} \cdot x_0}{F - F_{y2}} + L_s} & \text{(Region III)} \end{cases}$$

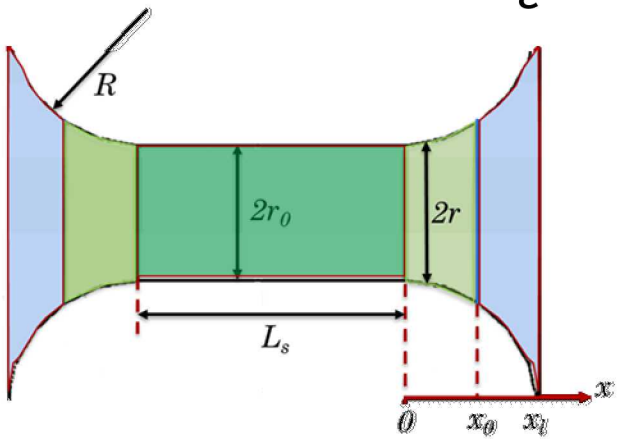

Experimental Output

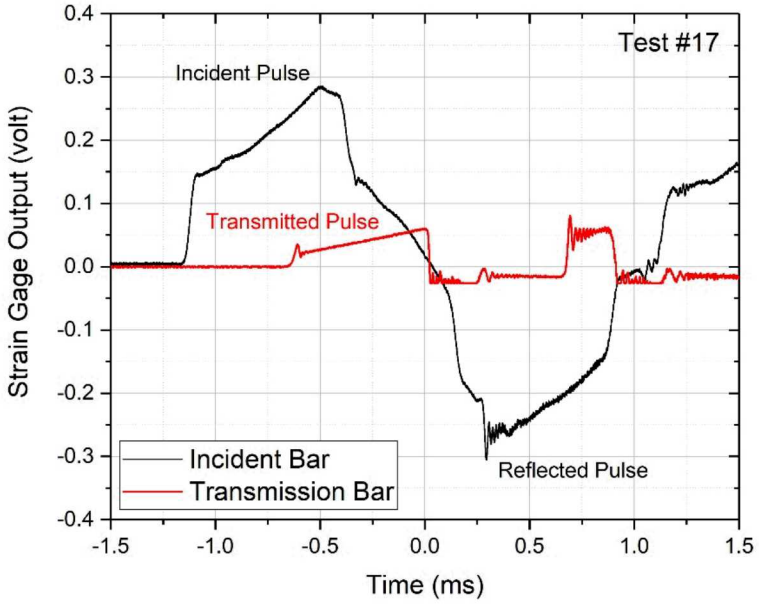

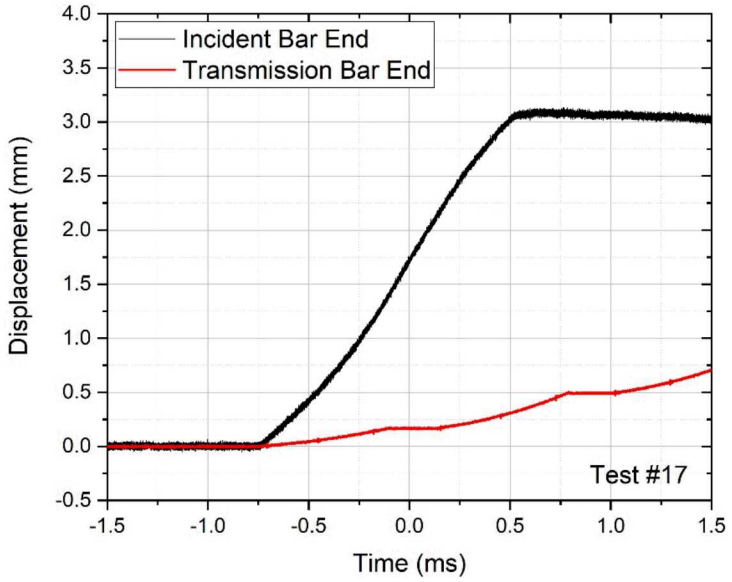

$$\sigma(t) = E_0 \cdot \varepsilon_t(t) \cdot \frac{A_0}{A_s}$$

$$\varepsilon = \begin{cases} c' \cdot \dfrac{L_1 - L_2}{L_s} & \text{(Region I)} \\ \dfrac{L_1 - L_2}{L_s} - \dfrac{F}{E_s \cdot \pi \cdot r_0^2} \cdot \left(\dfrac{1}{c'} - 1\right) & \text{(Region II)} \\ \dfrac{F_{y1}}{E_s \cdot \pi \cdot r_0^2} + \dfrac{L_1 - L_2 - \dfrac{2 \cdot F}{E_s \cdot \pi} \cdot \int_{x_0}^{x_1} \dfrac{dx}{\left(R + r_0 - \sqrt{R^2 - x^2}\right)^2} - \dfrac{F_{y1}}{E_s \cdot \pi \cdot r_0^2} \cdot (2x_0 + L_s)}{\dfrac{2 \cdot F \cdot r_0^2 \cdot \int_0^{x_0} \dfrac{dx}{\left(R + r_0 - \sqrt{R^2 - x^2}\right)^2} - 2 \cdot F_{y2} \cdot x_0}{F - F_{y2}} + L_s} & \text{(Region III)} \end{cases}$$

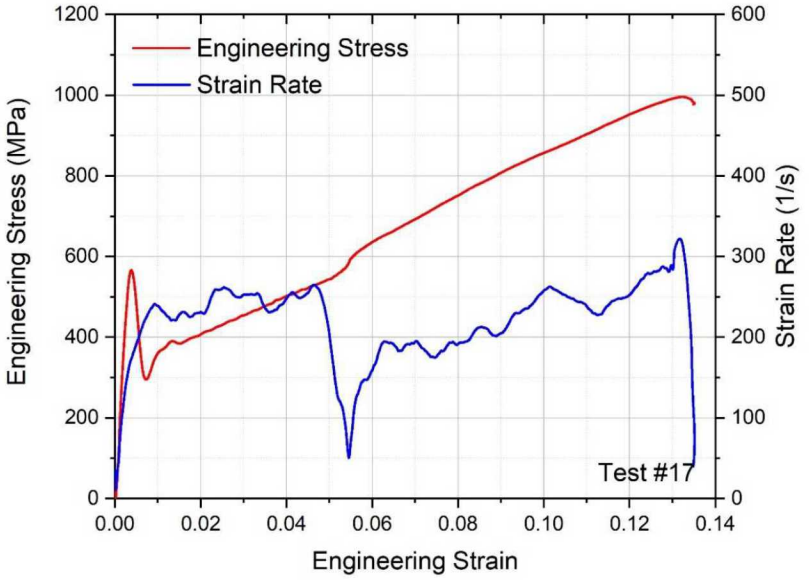

Stress-Strain Behavior

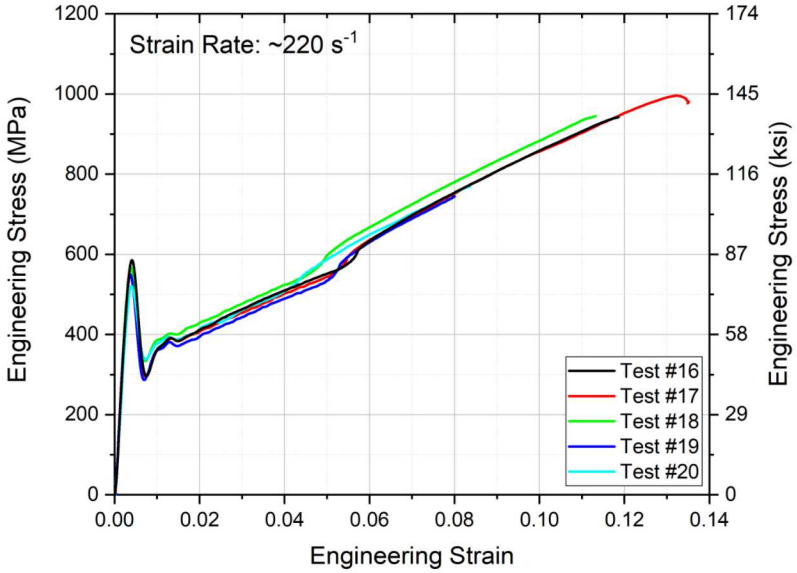

- SHPB
- Ambient temperature
- General behavior is similar for other temperatures (for same rate)

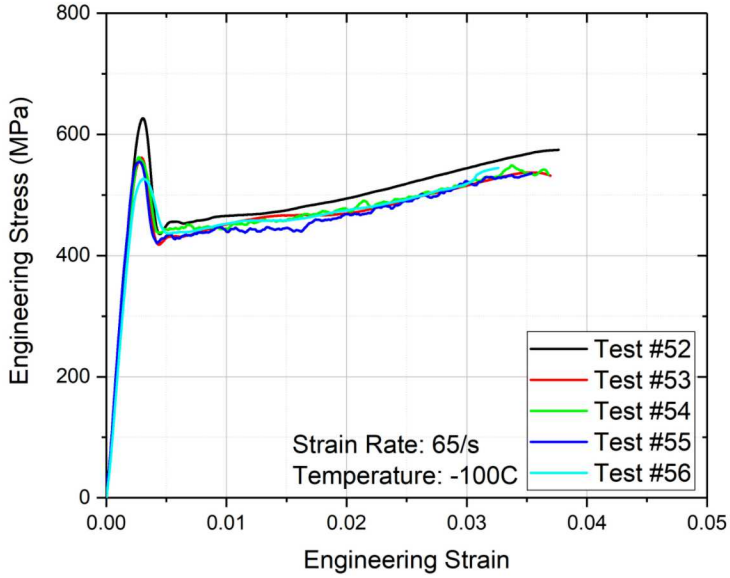

- SHPB
- -100°C
- 65/s (lower rate)

Stress-Strain Behavior

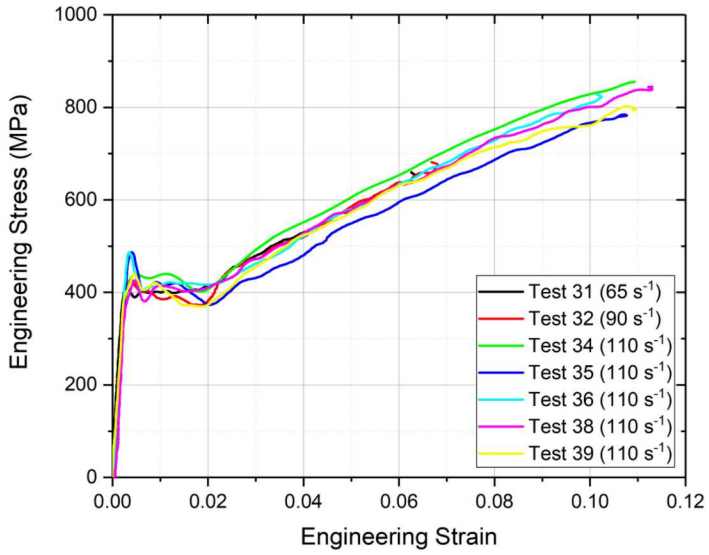

- DH Bar
- Ambient temperature
- 65-110/s
- Upper/lower yield becomes less pronounced

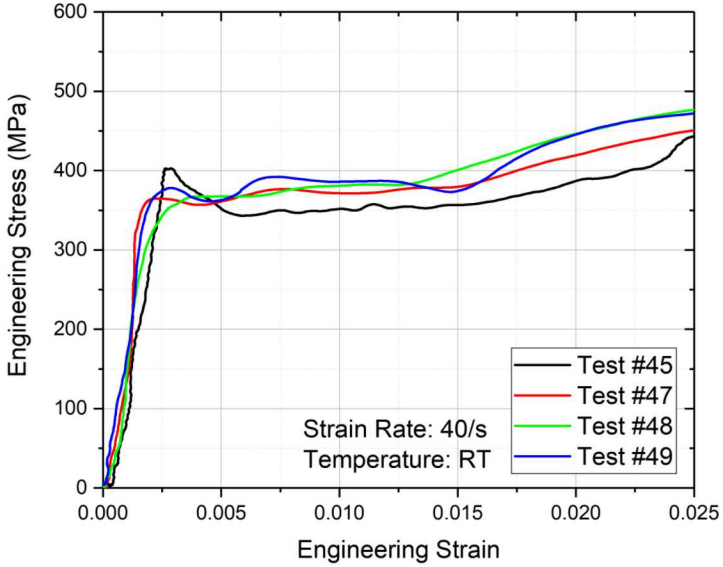

- DH Bar
- Ambient temperature
- 40/s
- Upper/lower yield becomes even less pronounced

Strain Rate Effects

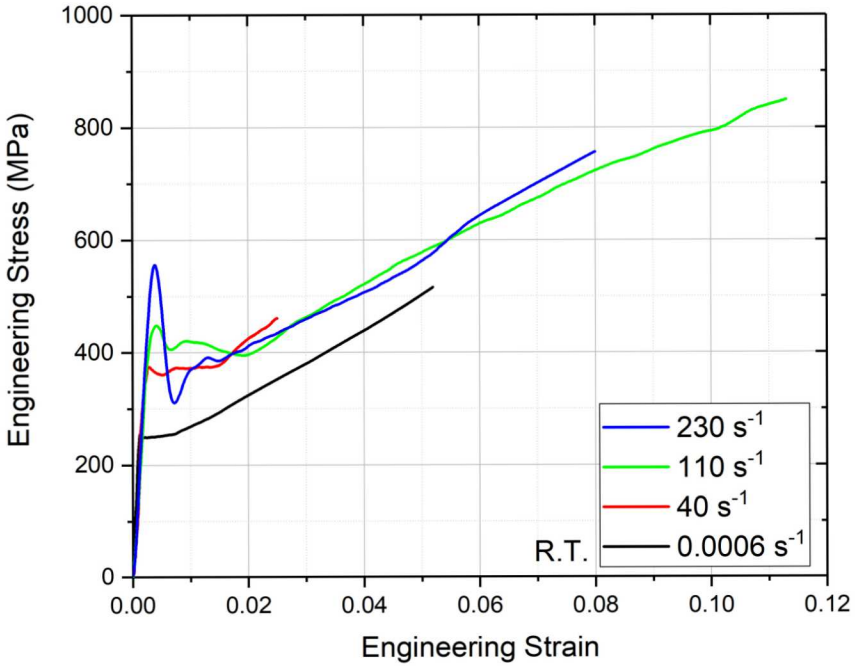

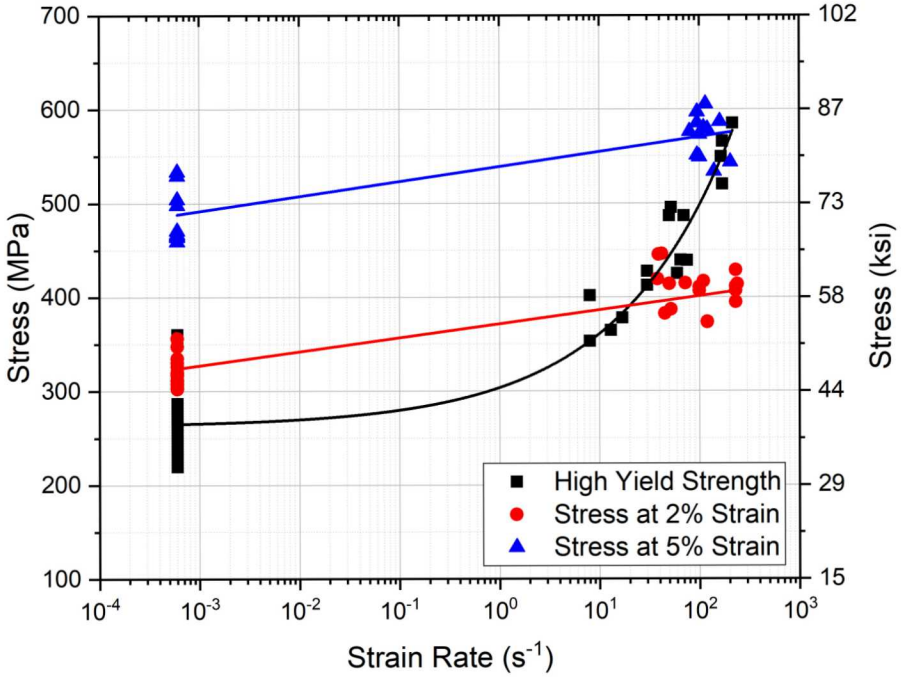

Temperature Effects

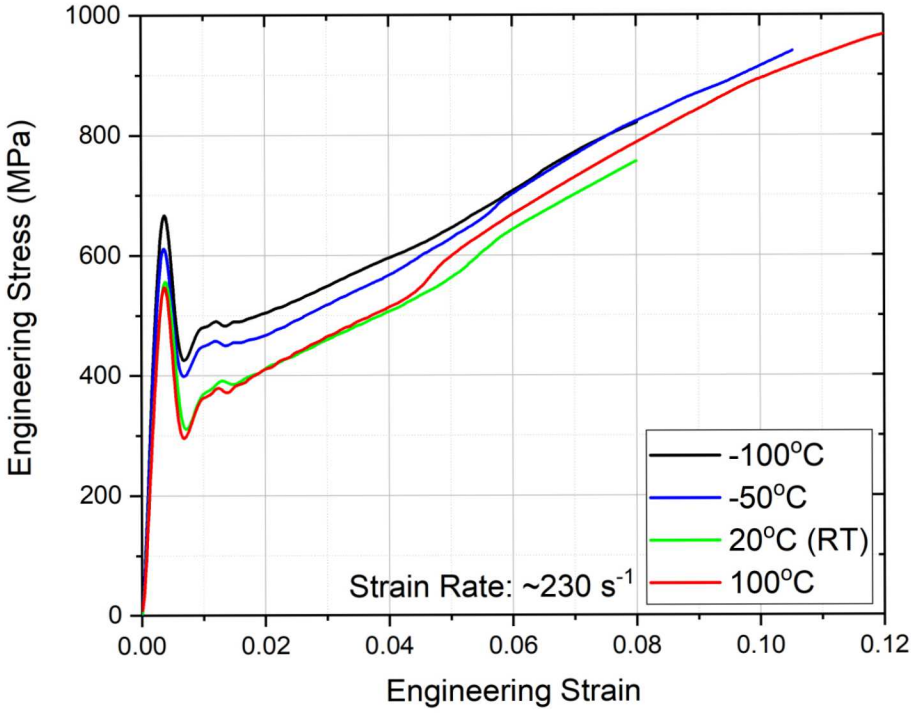

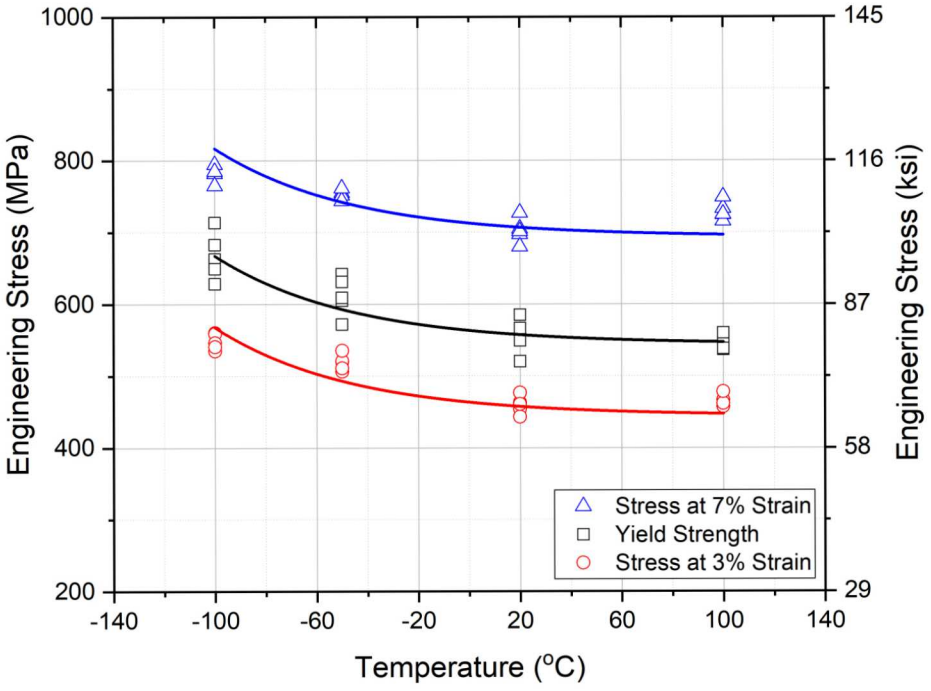

Temperature Effects

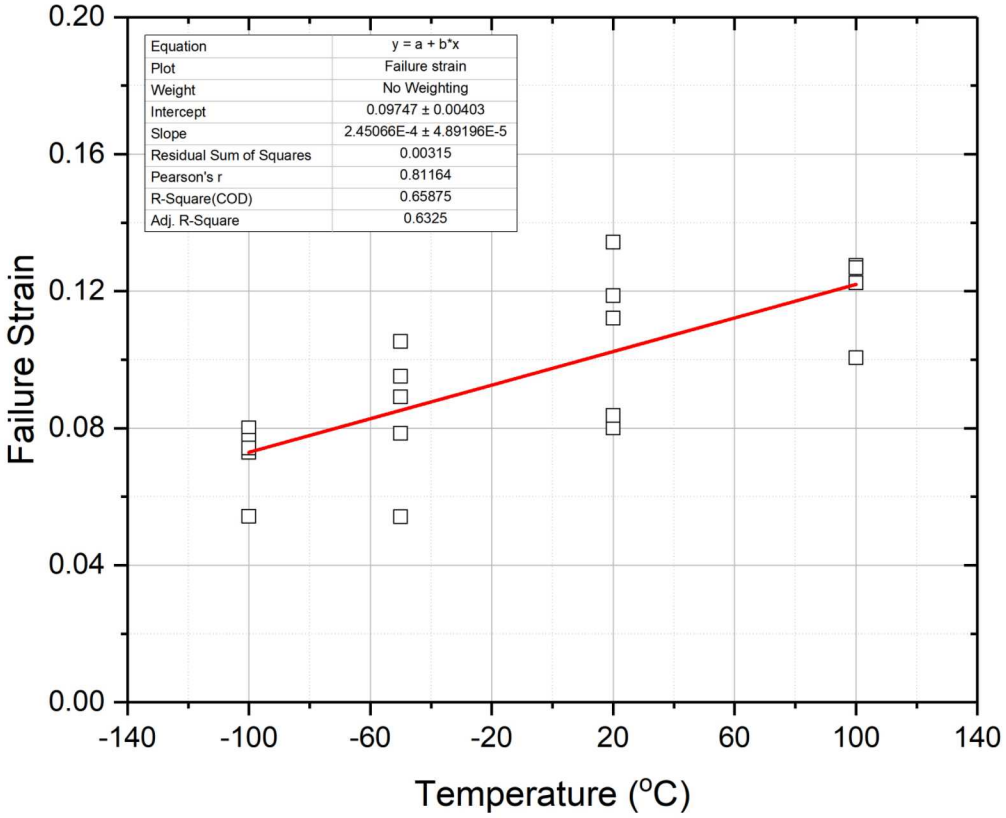

Fracture Morphology

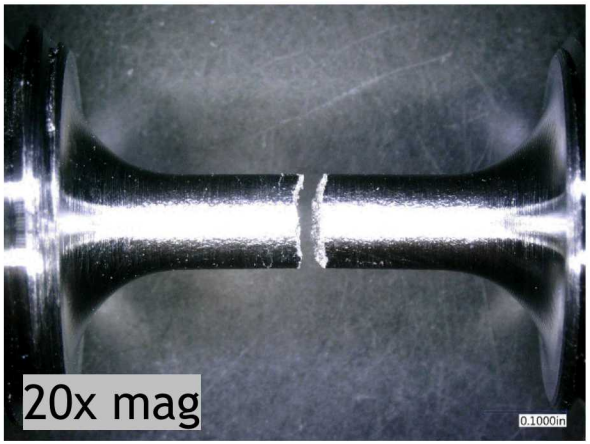

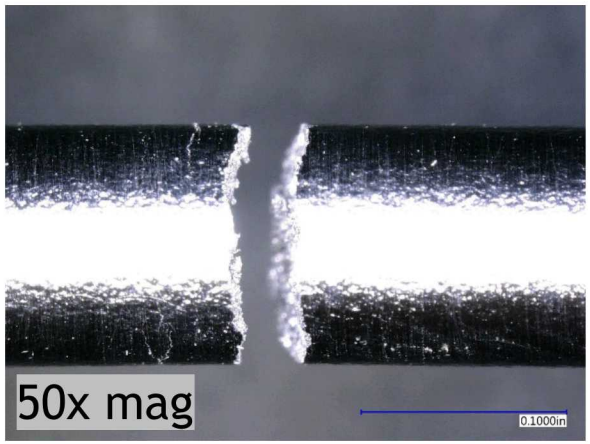

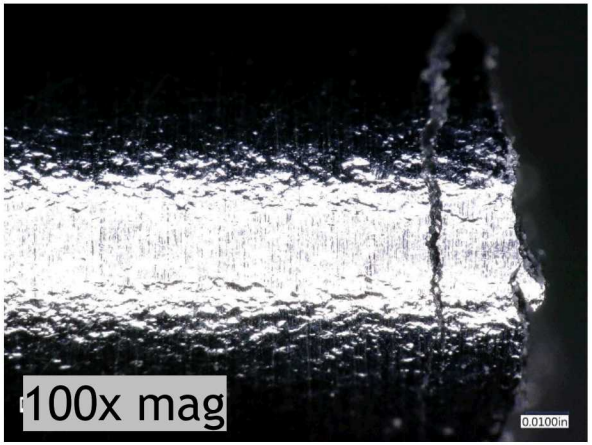

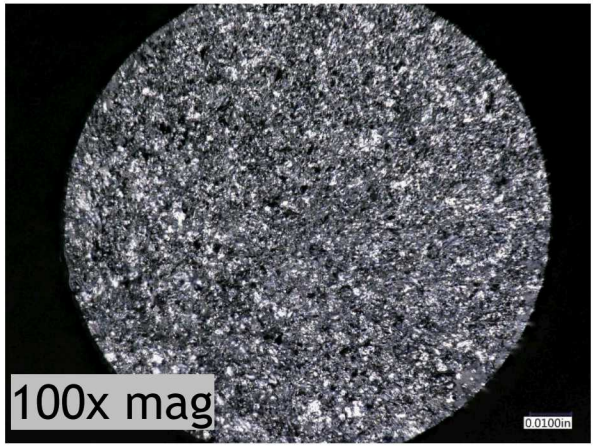

- No necking is evident
- Brittle fracture
- Specimens were round after failure (in-plane isotropic)
- Typical for all temperatures and rates

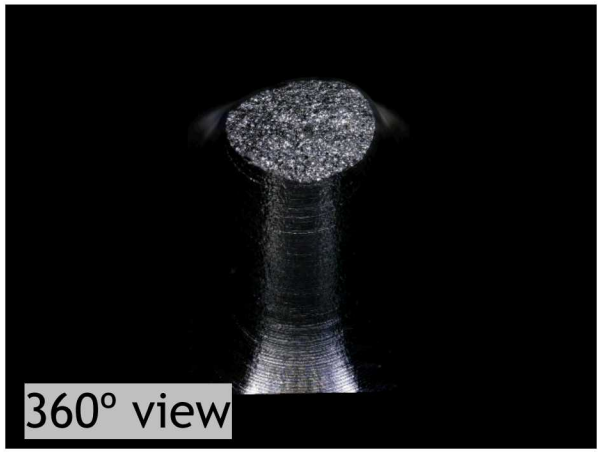

Conclusions

- Fe-Co-2V characterized using Drop-Hopkinson bar and Kolsky over wide range of temperatures and strain rates
- Stress-strain behavior had a linear elastic response followed by an upper and lower yield before linearly hardening to failure
- The upper/lower yield behavior decreased with decreasing strain rate
- Hardening rate was independent of strain rate or temperature (within the temperature range)
- Failure strain increased with increasing temperature
- Failure mode was brittle for all rates and temperatures
- All this information can be applied to a rate and temperature dependent constitutive model for this material